Hindawi Publishing Corporation
International Journal of Photoenergy
Volume 2012, Article ID 120214, 16 pages
doi:10.1155/2012/120214

Research Article

A Comprehensive Review and Analysis of Solar Photovoltaic Array Configurations under Partial Shaded Conditions

R. Ramaprabha and B. L. Mathur

Department of EEE, SSN College of Engineering, Kalavakkam-603 110, Chennai, India

Correspondence should be addressed to R. Ramaprabha, ramaprabhasuresh@gmail.com

Received 12 August 2011; Revised 17 November 2011; Accepted 19 November 2011

Academic Editor: Songyuan Dai

The aim of this paper is to investigate the effects of partial shading on energy output of different Solar Photovoltaic Array (SPVA) configurations and to mitigate the losses faced in Solar Photovoltaic (SPV) systems by incorporating bypass diodes. Owing to the practical difficulty of conducting experiments on varied array sizes, a generalized MATLAB M-code has been developed for any required array size, configuration, shading patterns, and number of bypass diodes. The proposed model which also includes the insolation-dependent shunt resistance can provide sufficient degree of precision without increasing the computational effort. All the configurations have been analyzed and comparative study is made for different random shading patterns to determine the configuration less susceptible to power losses under partial shading. Inferences have been drawn by testing several shading scenarios.

1. Introduction

Solar photovoltaic array is formed by series/parallel combination of SPV modules to attain a desired voltage and current level. The major challenge in using a SPV source containing a number of cells in series is to deal with its nonlinear internal resistance. The problem gets complex when the array receives nonuniform irradiance or partially shaded. In a larger SPVA, the occurrence of partial shading is common due to tree leaves falling over it, birds or bird litters on the array, shade of a neighboring construction, and so forth. In a series connected string of cells, all the cells carry the same current. Even though a few cells under shade produce less photon current, these cells are also forced to carry the same current as the other fully illuminated cells. The shaded cells may get reverse biased, acting as loads, draining power from fully illuminated cells. If the system is not appropriately protected, hot-spot problem [1] can arise and in several cases, the system can be irreversibly damaged. Nowadays there is an increasing trend to integrate the SPV arrays at the design level in the building itself. In such cases it is difficult to avoid partial shading of array due to neighboring buildings throughout the day in all the seasons. In conventional SPV systems, these shadows lower the overall generation power to a larger degree than what is expected. Hence the SPV installation cost is increased, because the number of SPV modules must be increased [2] and as a result, SPV power generation will be less attractive. This makes the study of partial shading of SPV modules a key issue. Moreover it is very important to understand the characteristics of SPVA under partial shaded conditions to use SPV installations effectively under all conditions.

In recent years, the impact of partial shading on the SPV array performance has been widely discussed [3–6]. With a physical SPV module it is difficult to study the effects of partial shading since the field testing is costly, time consuming and depends heavily on the prevailing weather conditions. Moreover, it is difficult to maintain the same shade under varying numbers of shaded and fully illuminated cells throughout the experiment. However it is convenient to carry out the simulation study with the help of a computer model. In most of the studies [7–10], the effect of partial shading in reducing the output power of the SPVA has been discussed. But little attention has been paid to the power dissipated by the shaded cells affecting the array life and utilization of the array for the worst shaded case. The

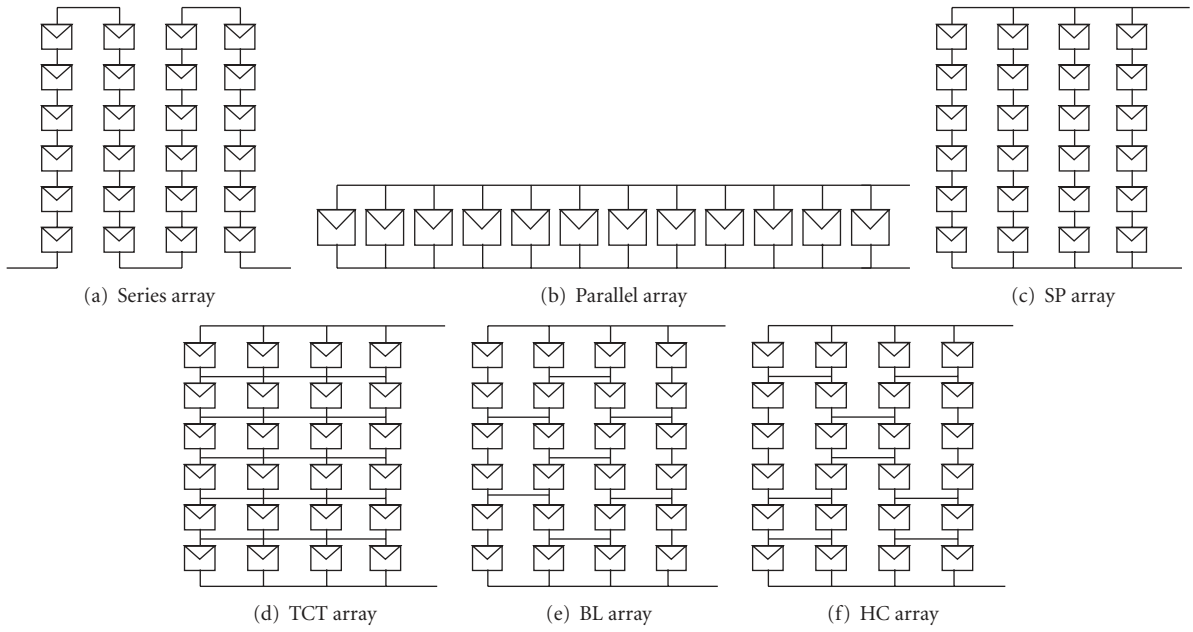

Figure 1: Schematic diagrams of SPVA configurations.

harmful effects in basic configurations and their comparison have been discussed in [11]. Common use of bypass diodes in antiparallel with the series-connected SPV modules can partially mitigate the power reduction due to partial shadow [11]. In such cases a more sophisticated Maximum Power Point Tracking (MPPT) algorithms capable to disregard local power maximums is required [12–16]. Alternatively, the maximum available DC power can be improved if the connection of the SPV modules can be reconfigured such that panels with similar operating conditions are connected in the same series string. Moreover the parallel configuration should be dominant under partial shaded conditions [11, 16–18]. However high output current at low voltage in parallel configuration will have to be properly conditioned to the required level by using suitable DC-DC converter. Hence it is required to opt for derived configurations. In this paper, for different configuration types, the generalized MATLAB programs have been developed which are capable of simulating any number of modules connected in series, parallel or combined for any type of shading patterns and any number of bypass diodes. The comparative study is made among the configurations and conclusions have been presented.

2. Review of Different SPVA Configurations

Several SPVA configurations have been proposed in the literature as shown in Figures 1(a) to 1(f) [1, 4, 19, 20]. They are series, parallel, series-parallel (SP) total cross-tied (TCT) bridge-linked (BL) and Honey-comb (HC) configurations [21, 22]. Series and parallel configurations are the basic configurations (Figures 1(a) and 1(b)) and the performance of these configurations has been discussed in detail by [11]. The major drawbacks of using the series or parallel configuration are that the current and voltage are less respectively. In SP configuration, shown in Figure 1(c) the modules are first connected in series to get the requisite voltage and then series-connected modules are paralleled. TCT configuration is derived from the SP configuration by connecting ties across rows of the junctions. In TCT configuration (Figure 1(d)), the voltages across the ties are equal. The sum of currents across the various ties is equal. The power is obtained as SP configuration. In BL configuration the modules are connected in a bridge rectifier fashion as shown in Figure 1(e). From the diagram it is seen that four modules constitute a bridge. Here two modules in the bridge are connected in series and then they are connected in parallel. Ties are present between the bridges. Hence the voltage and current values are obtained by appropriately adding voltages in series and currents in parallel.

The modifications have been made in BL configuration to arrive at a new configuration called HC configuration [21, 22]. The advantages of TCT and BL configurations have been combined together in HC configuration. Sometimes, insolation pattern on an array may be such that consecutive modules in a column of array receive equal insolation and other modules in a same column receive different insolation. In this case, it is not necessary to select TCT as it has so many ties. BL may also cause power loss as it has fewer ties in this case. So we have to select ties properly. This is obtained by connecting ties across variants of two, four, and six modules. This is done in HC configuration as shown in Figure 1(f) [21, 22].

3. Simulation of Configurations under Partial Shaded Conditions

Quaschning and Hanitsch [1] proposed a numerical algorithm to simulate the mismatch in individual SPV cells

and their shading levels. But it requires each element to be represented by a mathematical expression. Even though this produces accurate results, the model is complex and requires more computation time and higher memory requirement. Kaushika and Gautam [4] developed a computational network analysis approach to compare the configurations. Karatepe et al. [10] proposed a module-based and cell-based model for analyzing the array configurations. Giraud and Salameh [20] proposed a neural network-based model to investigate the effects of passing clouds on a grid-connected SPV system using battery storage. The importance of selecting the proper size of the SPV array and batteries in such systems has been discussed by [23]. It is required for the stable operation of SPV system with a sudden and large change in SPV power because of irradiance variation, caused by shading, and so forth. Shading caused due to passing clouds also has a financial claim on the utility. Jewell and Unruh [24] have carried out an economic analysis to estimate the cost of the fluctuations in power generation from a SPV source. Based on the literature it is understood that not only the size of the SPVA but also its configuration that significantly affects its power output, and therefore, the performance of the system under partially shaded conditions. From the above discussion, it may be concluded that, while it is very important to model, study, and understand the effects of shading on SPV arrays, a simple tool is not available for the purpose. Therefore, it is felt that there is a need for a flexible, interactive, and comprehensive simulation model capable to predict the SPV characteristics (including multiple peaks) and output power under partially shaded conditions. Patel and Agarwal [25, 26] have proposed a MATLAB based-simulator cum learning tool to understand the characteristics of a large SPV array by considering the model in I quadrant given in Figure 2. They have developed a model for SP configuration with bypass diodes. The model used by [25] neglects the effect of shunt resistance. Swaleh and Green [27] discussed the impact of R_{sh} under partial shaded conditions. In order to obtain the realistic model which provides the practical maximum power point values, it is mandatory to include the effect of varying R_{sh} with respect to environmental parameters particularly for crystalline type SPV modules. Hence the proposed model includes the insolation-dependent shunt resistance and the basic model equations used by [25] have been replaced by the improved model equations used by Villalva et al. [28]. The model equations (A.1)–(A.9) given in the appendix are used for modelling the SPV system. Equations (A.1) to (A.9) relating the SPV parameters with irradiance and temperature have been taken from [28] excluding (A.6). The parameters of (A.6) have been experimentally determined. The dependence of R_{sh} is found to be negligible and hence neglected to reduce the complexity of the model. The equations given in the appendix are for single SPV module.

Modeling of a large array with shading patterns is very complex. In this work, software has been developed for all the configurations having any number of assemblies, strings, substrings, and so forth. The software is capable of considering/ignoring the effect of varying insolation on R_{sh}. This software gives the output power, voltage, and current

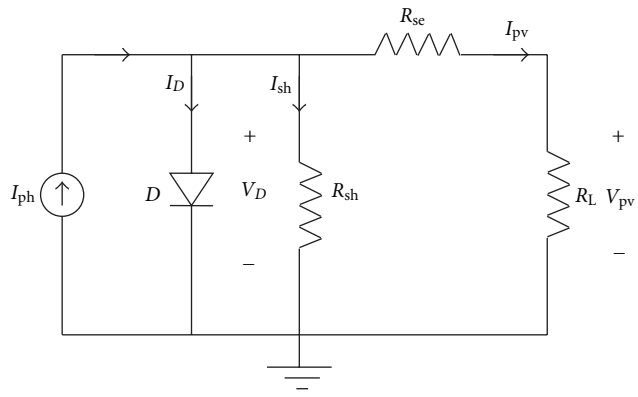

Figure 2: Electrical equivalent circuit model of a SPVA in I quadrant.

values for any irradiance and temperature patterns. Before going in detail about the software some of the terminologies are introduced with the help of Figure 3. Most of the SPV arrays in real time are large in size. It is cumbersome to enter the individual irradiance and temperature values for each module [25, 26]. Therefore groups of modules have been considered based on shading pattern. The representation of the terminologies has been explained with 6×4 array shown in Figure 3. The terminologies used in the proposed software are as following.

(i) Modules that always refer to a typical SPV panel consisting of a group of 36 cells connected in series. An antiparallel diode shunting 36/18 cells connected/ignored can be programmed.

(ii) Modules that are receiving the same irradiance connected in series form a "substring."

(iii) Several substrings that are receiving different irradiance but connected in series form a "string."

(iv) Identical strings that are connected in parallel form an "assembly."

(v) Assemblies that are connected in parallel form an "array."

As the importance of bypass diodes is well known, a bypass diode has been included as a part of every module in the M-file code. This section considers that each module is connected with a bypass diode. To include the effect of bypass diode, negative voltages caused by shading is taken as diode forward drop ($\sim$0.7 V) in M-file coding.

The architecture of the developed software is shown in Figure 4.

The individual block of Figure 4 is presented in the form of flow chart from Figure 5(a) to Figure 5(f). Figure 5(a) is common for all the configurations, after which there are subtle differences in the calculations of the various configurations. These are depicted from Figure 5(b) to Figure 5(f). The *V-I* and *V-P* characteristics for all the configurations including insolation-dependent R_{sh} is as shown in Figure 6 for a shading pattern shown in Figure 3. In the series configuration it is seen that the number of peaks correspond

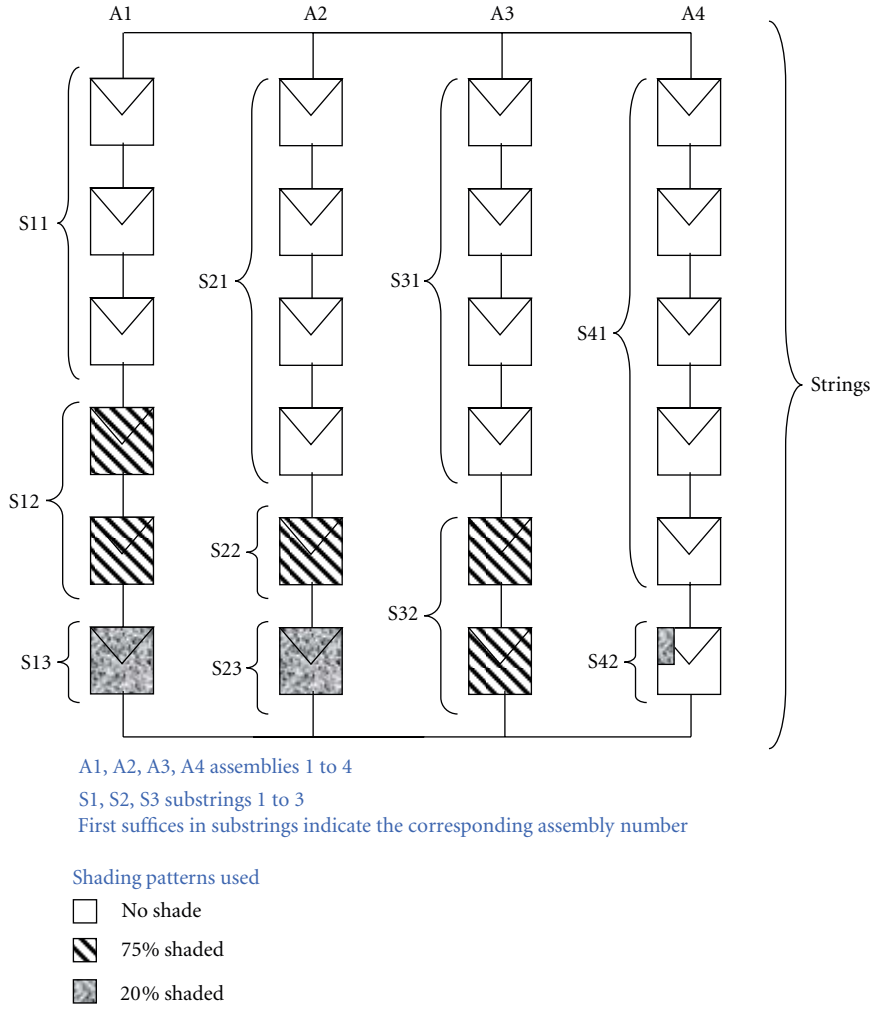

Figure 3: Illustration of 6×4 array with a particular shading pattern.

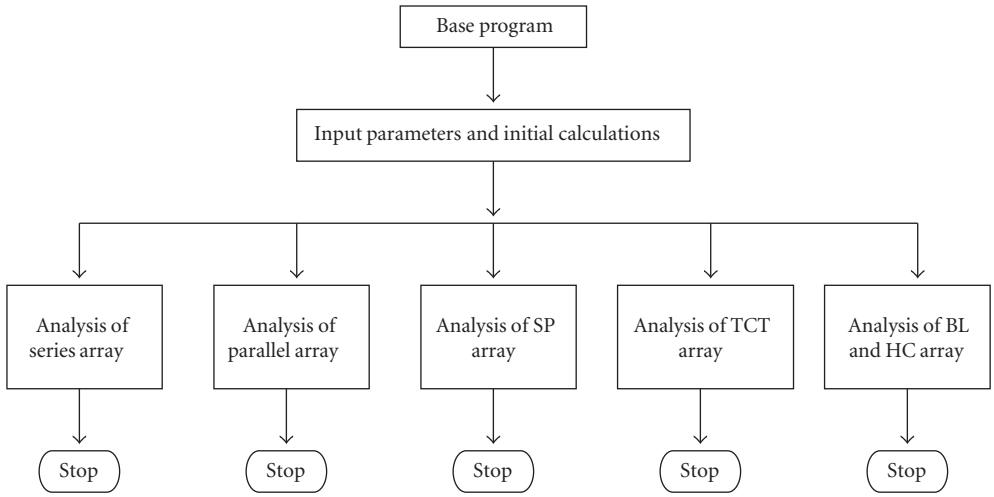

Figure 4: Architecture of the developed software.

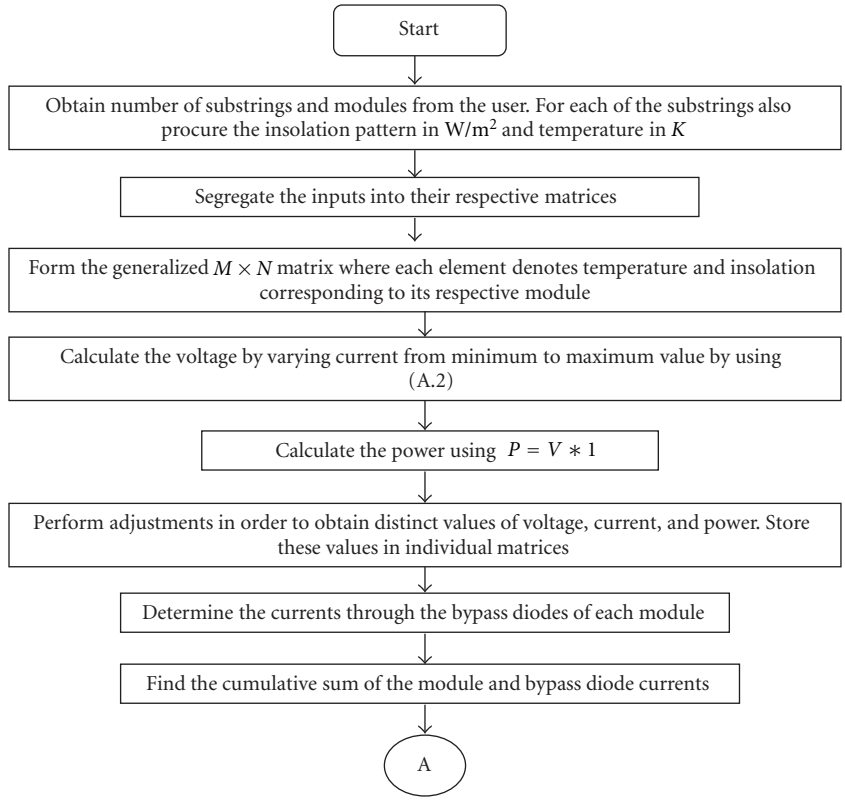

(a) Flow chart for initial part of all the configurations

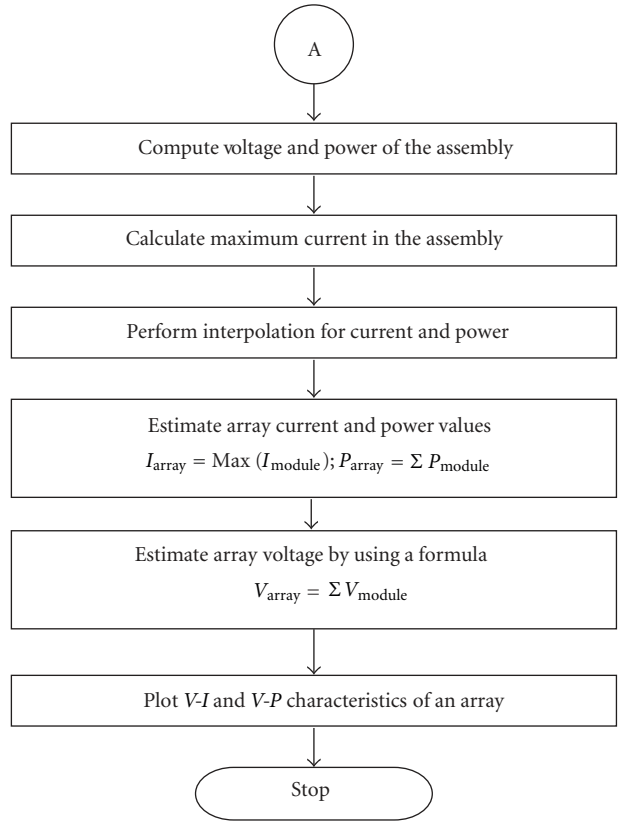

(b) Flow chart for Series configuration

Figure 5: Continued.

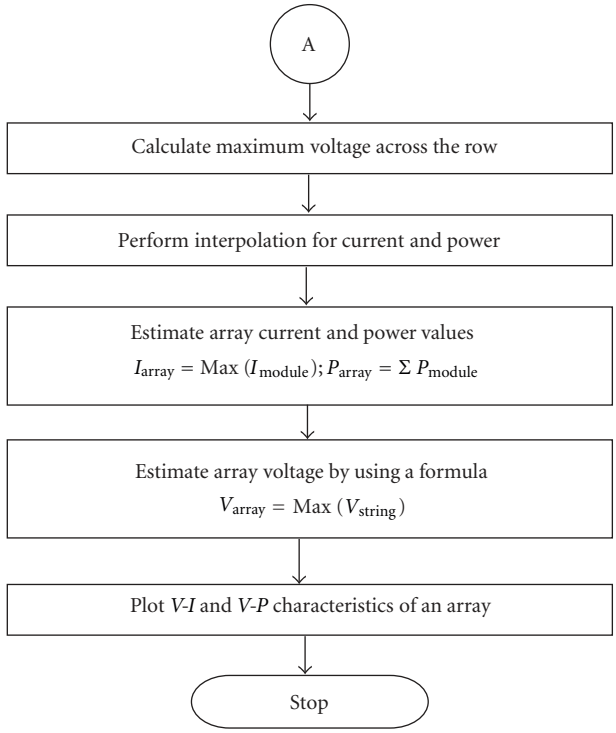

(c) Flow chart for parallel configuration

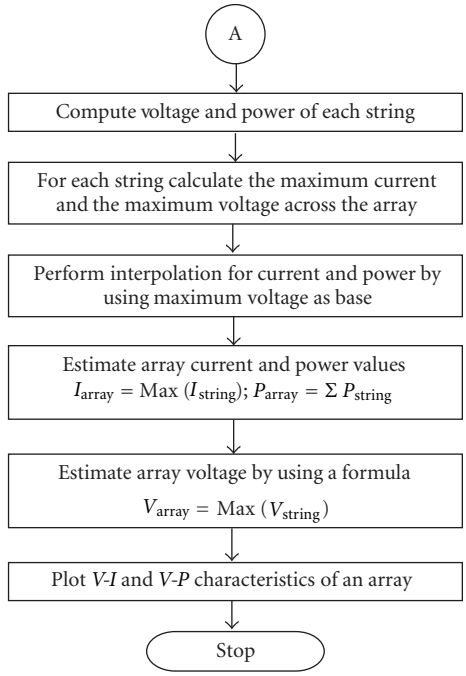

(d) Flow chart for SP configuration

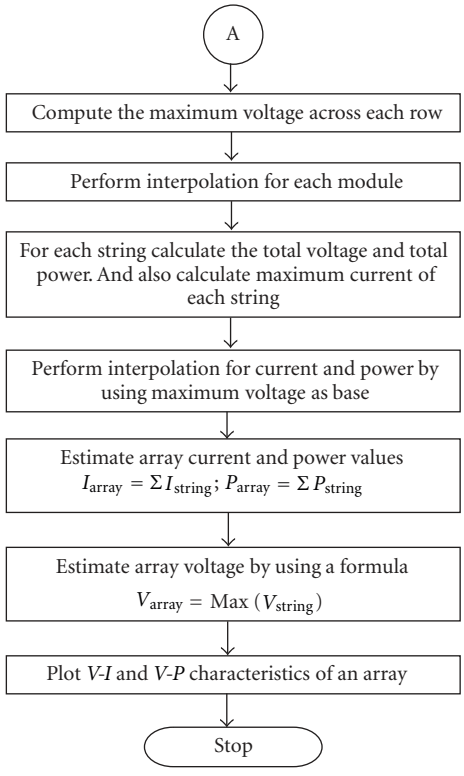

(e) Flow chart for TCT configuration

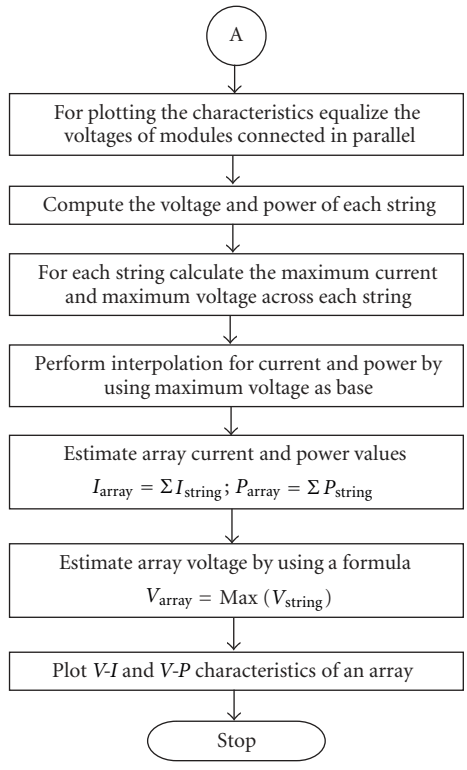

(f) Flow chart for BL and HC configurations (flow charts for BL and HC configurations are same but the ties have to be changed)

Figure 5: Flowchart for coding all the configurations.

Table 1: Comparison of power with and without the effect of insolation-dependent R_{sh}.

Configuration	P_m(W) constant R_{sh} (R_{sh} = 145.62 Ω)	P_m(W) with insolation-dependent R_{sh}
Series	**520.7**, 408.3, 193.1 (three peaks)	**488.2**, 387.8, 185.4 (three peaks)
Parallel	**564.8** (one peak)	**565.3** (one peak)
SP	421.6, 455.5, **458.9**, 370.5 (four peaks)	410.7, **435.8**, 434.2, 346.1 (four peaks)
TCT	341.4, 480.2, **551.6**, 416.4 (four peaks)	443.5, **468.4**, 463.3, 372.7 (four peaks)
BL	362.7, 479.6, **483.1**, 447.8 (four peaks)	410.7, **435.8**, 433.5, 393.1 (four peaks)
HC	428.1,445.2, **448.7**, 418.3 (four peaks)	394.3, 436.1, **442.8**, 385.6 (four peaks)

Table 2: Comparisons of Configurations under Uniform Irradiance Conditions.

Configuration	P_m(W)	V_m(V)	I_m (A)
Series	676.8	292.1	2.32
Parallel	676.8	12.26	55.2
SP	676.8	73.05	9.27
TCT	676.8	73.05	9.27
BL	676.8	73.05	9.27
HC	676.8	73.05	9.27

to the number of shading patterns and current is less compared with other configurations. In this configuration it is understood that if even one module is shaded it affects the output power considerably. In the parallel configuration it is seen that there are no multiple peaks. This is because all the modules are connected in parallel; therefore no module can be forced to carry more than its share of current. In parallel configuration the voltage is less. SP configuration provides higher power at considerable voltage and current values. Hence it can be inferred that SP configuration negates the defects of series and parallel configurations. In TCT configuration due to the inclusion of ties, the flaws of the series configuration have been avoided. This is because none of the modules are connected in series. Hence stress on modules is reduced. In BL configuration few modules in a string are connected in series and these are connected in parallel. Therefore it subjected to lesser stress than SP configuration. The generalized MATLAB program has been extended for HC with modifications. The flowchart for HC configuration is similar to BL. While writing the program the difference in the tie connections has been taken care of (Figure 5(f)).

4. Impact of Including the Effect of Varying Shunt Resistance in the Model

Table 1 shows the comparison between power values with and without the varying shunt resistance. The input pattern is given as shown in Figure 3. It is seen that the power values change when varying shunt resistance is included. The power values in the third column of Table 1 matches very closely with practical values. Hence shunt resistance should be included in order to obtain the realistic modeling of SPV array.

5. Comparison of Array Configurations with and without Bypass Diode

For the analysis of array configurations without bypass diode, two quadrant characteristics have to be taken care of. [29, 30]. Hence the additional term is included in the mathematical model as shown in Figure 7 [31] and the same set of programs has been modified with the model represented by (A.10). Table 2 shows the power, voltage, and current values under uniform irradiance conditions. This corresponds to an irradiance of 1000 W/m^2 and a temperature of 25°C (298.15 K). It is seen that almost all the configurations provide the same power under uniform irradiance conditions.

Table 3 shows the comparison of power with and without a bypass diode for a 6 × 4 array. The input pattern is as in Figure 3. Even though the use of bypass diode introduces multiple peaks, it is seen from Table 3 that a higher power is obtained by using a bypass diode.

6. Comparison of Different Array Configurations for Different Shading Scenarios

Here the case where one bypass diode across a group of 36 cells (one bypass diode per module) has been considered. The array sizes are 2 × 4, 4 × 2, 2 × 6, 6 × 2, 3 × 4, 4 × 3, 4 × 6, 6 × 4, 3 × 3 and 4 × 4. An array size can be designated by $M \times N$, where M indicates number of modules connected in series and N indicates number of strings in parallel. Fifteen different random shading patterns are generated for each of the ten different array sizes. One of the 15 random patterns of irradiance is shown in Figure 8 and corresponding shading matrix for different array sizes are shown in Figure 9. In Figure 8, the shading patterns E, L, R, and X are very low values which replicate the bird litters or single leaves closing completely the cell in a larger array. Practically it is found that some of the bird litters are difficult to remove from the array which causes permanent shade on the cell so that particular cell receives very low insolation at all times. The maximum power obtainable from each configuration is computed for each of these shading patterns. The mean value of this power and its maximum and minimum values for different shading patterns have been tabulated vide Table 4 in which the values highlighted with bold letters indicate the global peak values whereas other values are local peak values.

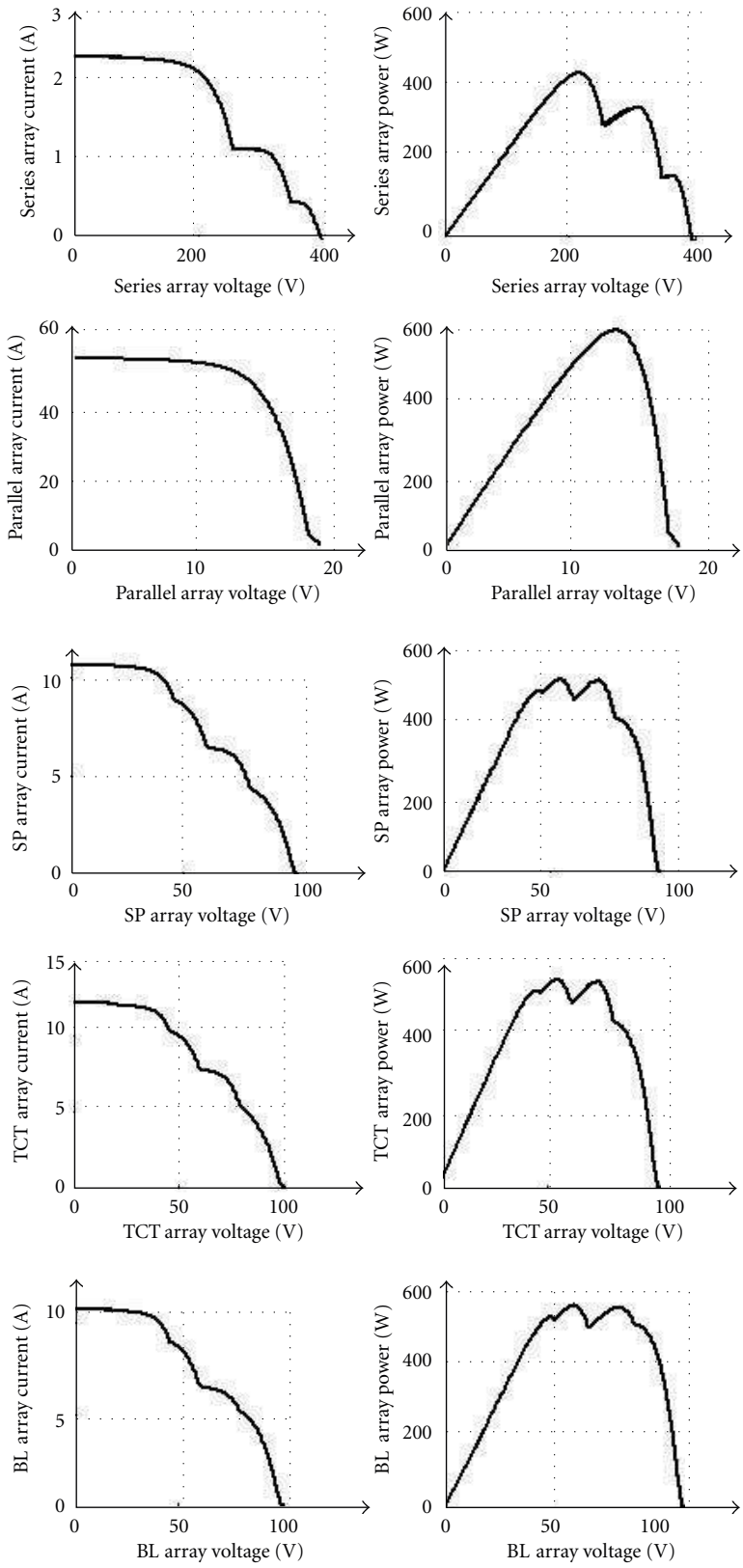

Figure 6: Continued.

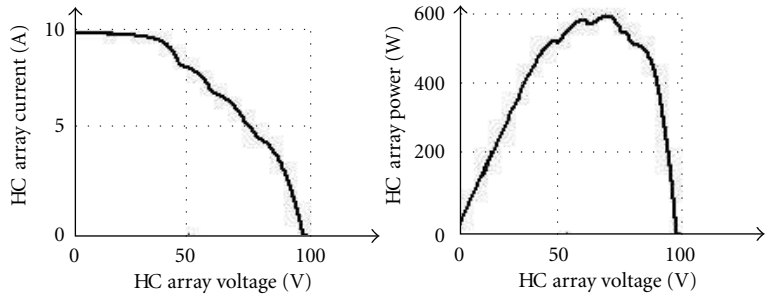

Figure 6: Simulated *V-I* and *V-P* characteristics of SPVA configurations for a shading pattern shown in Figure 3.

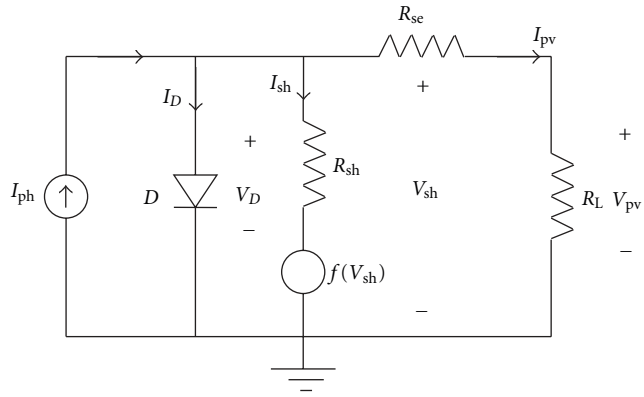

Figure 7: Bishop's model to represent the SPVA under partial shaded condition.

From Table 4 it can be inferred that depending on the size of array and type of shading pattern different configurations are preferred. But in most of the cases TCT closely followed by HC are the preferred configurations. It is observed that wherever the modules with similar shade are grouped in a string, HC is better in which less ties are there as compared to TCT.

7. Practical Verification

A few results obtained from the software were verified. Figure 10 shows a set up of 3×3 SPV array. SOLKAR (Model No. 3712/0507) solar module is used to setup the array.

The electronic load [30] was used to verify the characteristics. GWINSTEK GDS-1022 DSO was used to trace the practical characteristics. It is calibrated using Fluke 5500 A Multi-Product Calibrator. For different irradiances and temperatures the practical characteristics are easily traced out using electronic load method and the relevant data traced by DSO are stored in Excel spreadsheet to calculate *V-P* characteristics and for comparison of model parameters. Solar irradiance level/insolation of 1000 W/m^2 corresponds to a short circuit current of 2.55 A as per the datasheet of SOLKAR modules. In all the experiments the solar insolation has been measured as proportional to short circuit current. Outputs were verified for uniform as well as partial shaded conditions. The sample snapshot of digital storage oscilloscope has been shown in Figure 10 for the four types of configurations (SP, TCT, BL, and HC) for a particular shading pattern. The calculated *P-V* characteristics for Figure 11 are shown in Figure 12. The practical verification was done for several artificially introduced input shading patterns. The outputs obtained were closer to the outputs obtained from simulation which took into consideration the effect of varying R_{sh}. Irradiance level of a module was assumed proportional to the short circuit current and different shadows were introduced by tilting the module of the stand.

8. Effect of Using More Bypass Diodes

The concept of using bypass diode is extended in this section. One diode is connected across a group of 18 cells in a module (2 bypass diodes per module) is considered. Table 5 gives the comparison between mean value of the power for 6×4 configurations with one bypass per module and two bypass diodes per module for fifteen random shading patterns.

From Tables 5 and 6, it is observed that the improvement in the power when two bypass diodes are used in the single module. This study can be extended to select the optimum number of diodes used in a module to get the maximum power under partial shaded conditions. If the number of bypass diodes used in a module is increased or in other words the number of cells grouped is minimized, the maximum output can be obtained.

The generalized program developed has been used to choose the optimum array configuration for the 10.5 kW array installed in the SSN research center (14×10 array)

Table 3: Comparison of Configurations Power with and without Bypass Diode.

Configuration	P_m(W) (without bypass diode)	P_m(W) (with bypass diode)
Series	325.52	**488.2**, 387.8, 185.4 (Three Peaks)
Parallel	557.2	**565.3** (one peak)
SP	408.08	410.7, **435.8**, 434.2, 346.1 (Four Peaks)
TCT	448.97	443.5, **468.4**, 463.3, 372.7 (Four Peaks)
BL	428.98	410.7, **435.8**, 433.5, 393.1 (Four peaks)
HC	440.78	394.3, 436.1, **442.8**, 385.6 (Four Peaks)

Table 4: Mean and Range of the maximum power for different configurations with different sizes under random shading patterns (*Readings practically verified vide Section 7).

Array Size	Configuration	Mean Value of Maximum Power (W)	Range of Maximum Power (W)	
			Maximum Value	Minimum Value
2 × 4*	SP	93.32	130.8	45.68
2 × 4*	TCT	94.67	131.40	45.43
2 × 4*	BL	105.58	161.90	47.61
2 × 4*	**HC**	**121.98**	**191.30**	**52.45**
4 × 2*	SP	103.96	154.30	54.80
4 × 2*	**TCT**	**117.70**	171.50	65.97
4 × 2*	BL	104.00	154.30	54.80
4 × 2*	HC	114.02	173.80	56.15
2 × 6	SP	145.51	217.40	83.43
2 × 6	TCT	149.78	239.40	95.20
2 × 6	BL	175.42	269.90	126.50
2 × 6	**HC**	**187.23**	**279.01**	**131.90**
6 × 2	SP	143.13	187.60	82.37
6 × 2	TCT	160.09	209.20	96.73
6 × 2	BL	143.11	187.80	82.27
6 × 2	**HC**	**165.34**	**215.90**	**84.11**
3 × 4	SP	128.14	190.50	62.96
3 × 4	TCT	142.58	207.00	84.04
3 × 4	**BL**	**146.70**	**205.60**	**67.86**
3 × 4	HC	144.93	226.80	66.93
4 × 3	SP	125.79	201.20	43.28
4 × 3	TCT	132.37	209.08	61.02
4 × 3	BL	132.89	226.40	73.70
4 × 3	**HC**	**137.95**	**225.10**	**55.31**
3 × 3*	SP	85.72	135.20	51.33
3 × 3*	**TCT**	**92.79**	145.70	54.58
3 × 3*	BL	84.50	135.20	46.94
3 × 3*	HC	83.22	128.60	53.73
4 × 4	SP	145.31	250.10	93.72
4 × 4	**TCT**	**164.62**	272.80	91.33
4 × 4	BL	145.03	225.80	93.72
4 × 4	HC	144.14	225.40	85.17
4 × 6	SP	186.66	302.10	131.97
4 × 6	TCT	211.54	375.47	146.56
4 × 6	BL	186.06	317.32	104.47
4 × 6	**HC**	**227.06**	**392.47**	**117.29**
6 × 4	SP	197.86	324.12	110.47
6 × 4	**TCT**	**234.57**	**383.12**	**113.29**
6 × 4	BL	184.48	334.36	98.65
6 × 4	HC	219.15	387.93	98.97

Pattern label	A	B	C	D	E	F	G	H	I	J	K	L	M	N	O	P	Q	R	S	T	U	V	W	X
Irradiance in W/m^2	355	259	657	780	29	667	352	627	618	310	994	42	196	420	902	468	263	97	602	643	814	829	492	79

Figure 8: One of the 15 random patterns of irradiance.

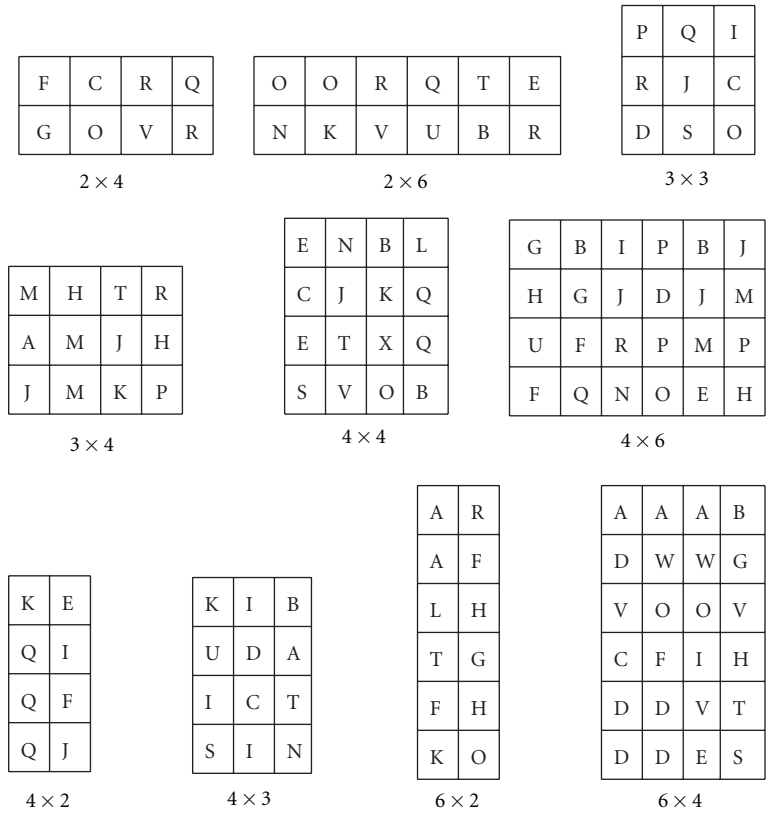

Figure 9: Shading matrixes for different array sizes with shading pattern of Figure 8.

Table 5: Comparison between mean value of the maximum power for 6 × 4 configurations with one bypass diode and two bypass diodes per module under random shading patterns.

Array size	Configuration	Mean value of maximum power (W)		Difference in mean value of power (W)
		One diode per module	Two diodes per module	
6 × 4	SP	197.86	218.87	21.01
6 × 4	**TCT**	**234.57**	**262.20**	**27.63**
6 × 4	BL	184.48	206.20	21.72
6 × 4	HC	219.15	245.60	26.45

Table 6: Deviation of RMSD and mean value for 6 × 4 array when one bypass diode across the module and two bypass diodes across two groups of 18 cells in the module.

Array size	Configuration	Maximum power (W)		Voltage at MPP (V)	
		Mean value	RMSD value	Mean value	RMSD value
6 × 4	SP	21.01	59.38	6.35	2.25
6 × 4	TCT	28.28	51.83	2.61	5.70
6 × 4	BL	22.68	57.71	4.77	2.91
6 × 4	HC	26.72	53.83	4.55	4.01

Table 7: Mean value and range of maximum power for 14 × 10 configuration shown in Figure 12.

Array size	Configuration	Mean value of maximum power (W)	Range of maximum power (W)	
			Maximum value	Minimum value
14 × 10	SP	2462.51	3289.00	1777.12
14 × 10	TCT	2628.83	3396.14	2054.37
14 × 10	BL	2561.17	3309.34	1876.46
14 × 10	**HC**	**2675.17**	**3562**	**2023**

Figure 10: Practical setup of a 3×3 array employing tilting modules for different shades.

Table 8

S. no	Parameters	Values
1	Rated power (P)	37.08 W
2	Voltage at maximum power (V_m)	16.56 V
3	Current at maximum power (I_m)	2.25 A
4	Open circuit voltage (V_{oc})	21.24 V
5	Short circuit current (I_{sc})	2.55 A
6	No. of series cells (N_s)	36
7	Type	Monocrystalline

which is shown in Figure 13. In this array for each module 18 cells are grouped together and bypass diode is connected in anti-parallel with that. In the generalized program the specifications according to the datasheet of BEL laboratories and the array size have been altered for the study. For this case, the maximum power is about 10.5 kW at maximum voltage and about 65.69 V under uniform irradiance condition (at $G = 1000\,\text{W/m}^2$ and $T = 25^\circ\text{C}$). The rated power per module is 75 W.

Table 7 gives the comparison of different array configurations under 20 random shading patterns. It is found that the HC configuration is dominated under partial shaded condition for the existing array.

9. Conclusion

Analysis of various SPVA configurations with respect to environmental parameters by developing a more realistic model using MATLAB M-file has been presented. In analysis a recent configuration, HC configuration, has also been taken for comparison. In order to obtain the maximum possible power under partial shaded conditions it is mandatory to connect a bypass diode in anti-parallel with a module or group of cells to avoid the stress on the shaded cells. This setup would reduce the problems of hot-spot as well as provide a higher power when compared to a SPVA without bypass diode. After analyzing the various configurations for different random shading patterns for varied sizes, it is also observed that in most cases TCT gave a higher amount of power when compared to the other configurations but in some cases where the array was asymmetrical or where the number of columns receiving same insolation was more when compared to the number of rows, HC configuration provided a higher power when compared to the other configurations because of less ties. Hence we can conclude that TCT is the best configuration closely followed by HC. After analyzing various configurations, it can be concluded that TCT is the best configuration for symmetrical array size and HC configuration for asymmetrical array sizes. The generalized program developed here can be used for any array size, any number of bypass diodes across group of cells, and for any module by simply changing the specifications of the module used in the program. Moreover, the results confirm that this approach often allows attaining a higher electrical energy production compared to that attainable with SPV arrays with a proper layout.

Appendix

The equations used to develop a simulation model of a SPV cell are: [28–31]

$$I_{PV} = I_{ph} - I_r\left[\exp\left\{\frac{V_{PV} + I_{PV}R_{se}}{V_t}\right\} - 1\right] - \frac{(V_{PV} + I_{PV}R_{se})}{R_{sh}}. \tag{A.1}$$

For coding purpose (A.1) has been rearranged as

$$V_{PV} = \ln\left\{\frac{I_{ph} - I_{PV} - (V_{PV} + I_{PV}R_{se})/R_{sh} + I_r}{I_r}\right\} \times V_t - I_{PV}R_{se}, \tag{A.2}$$

where

$$I_{ph} = \left\{I_{ph,ref}[1 + \alpha(T - T_{ref})]\right\}\frac{G}{G_{ref}},$$
$$I_{ph,ref} = I_{sc,ref}, \quad I_{ph,ref} = \frac{R_{sh} + R_{se}}{R_{sh}} \times I_{sc,ref}, \tag{A.3}$$

$$I_r = \frac{I_{sc,ref} + \alpha(T - T_{ref})}{\exp\left((V_{oc,ref} + \beta(T - T_{ref}))/nV_T\right) - 1},$$
$$I_{r,ref} = \frac{I_{sc,ref}}{\exp\left(V_{oc,ref}/V_{t,ref}\right) - 1}, \tag{A.4}$$

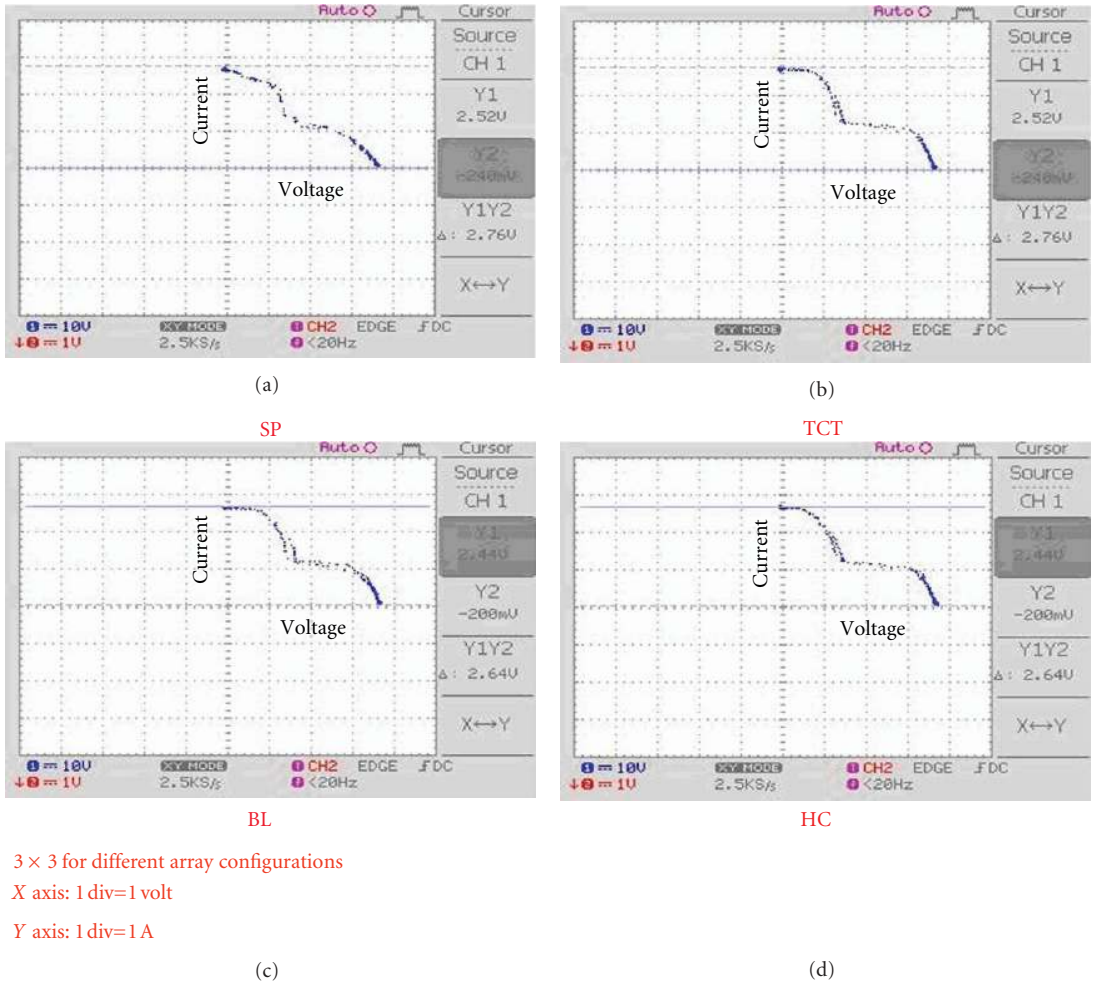

Figure 11: Snapshot of *I-V* characteristics for a 3 × 3 SPVA for different configurations.

$$V_t = V_{t,ref}\frac{T}{T_{ref}}, \qquad V_{t,ref} = \frac{n_{ref}kT_{ref}}{q} \tag{A.5}$$

$$R_{sh} = \frac{3.6}{G - 0.086}, \tag{A.6}$$

$$I_m = I_{m,ref} \times G, \qquad V_m = V_{m,ref} + \{\beta(T - T_{ref})\}, \tag{A.7}$$

$$R_{se}\frac{G}{G_{ref}} = \frac{V_{t,ref}}{I_{r,ref}}e^{-(V_{m,ref}+I_{m,ref}R_{se,ref})/V_{t,ref}} + R_{se,ref} - \frac{G}{G_{ref}}\left(\frac{V_t}{I_r}e^{-(V_m+I_mR_s)/V_t} + R_{se}\right), \tag{A.8}$$

$$n = n_{ref}\frac{T}{T_{ref}}, \tag{A.9}$$

The electrical behavior of the solar cell can be described by

$$I_{PV} = I_{ph} - I_r\left[\exp\left\{\frac{V_{PV} + I_{PV}R_{se}}{V_t}\right\} - 1\right] - \frac{(V_{PV} + I_{PV}R_{se})}{R_{sh}} - a\frac{(V_{PV} + I_{PV}R_{se})}{R_{sh}}\left(1 - \frac{V_{PV} + I_{PV}R_{se}}{V_{br}}\right)^{-m}, \tag{A.10}$$

where V_{br}: junction break down voltage, a: fraction of ohmic current involved in avalanche breakdown, and m: avalanche break down exponent.

The electrical behavior of the solar cell can be described by (A.10) over the whole voltage range. The unknown parameters are "a", "V_{br}", and "m". These parameters are calculated by extracting parameters in those areas of practical *V-I* characteristic which are more significant.

The *V-I* characteristics of the solar cell under reverse biased conditions for dark condition have been measured. Breakdown voltage is calculated by linear regression of the straight line of voltage against the inverse of current near breakdown region from the dark characteristics [32]. The breakdown voltage V_{br} of the cell is found to be 13.5 V. The other two parameters are found by tuning them in model by

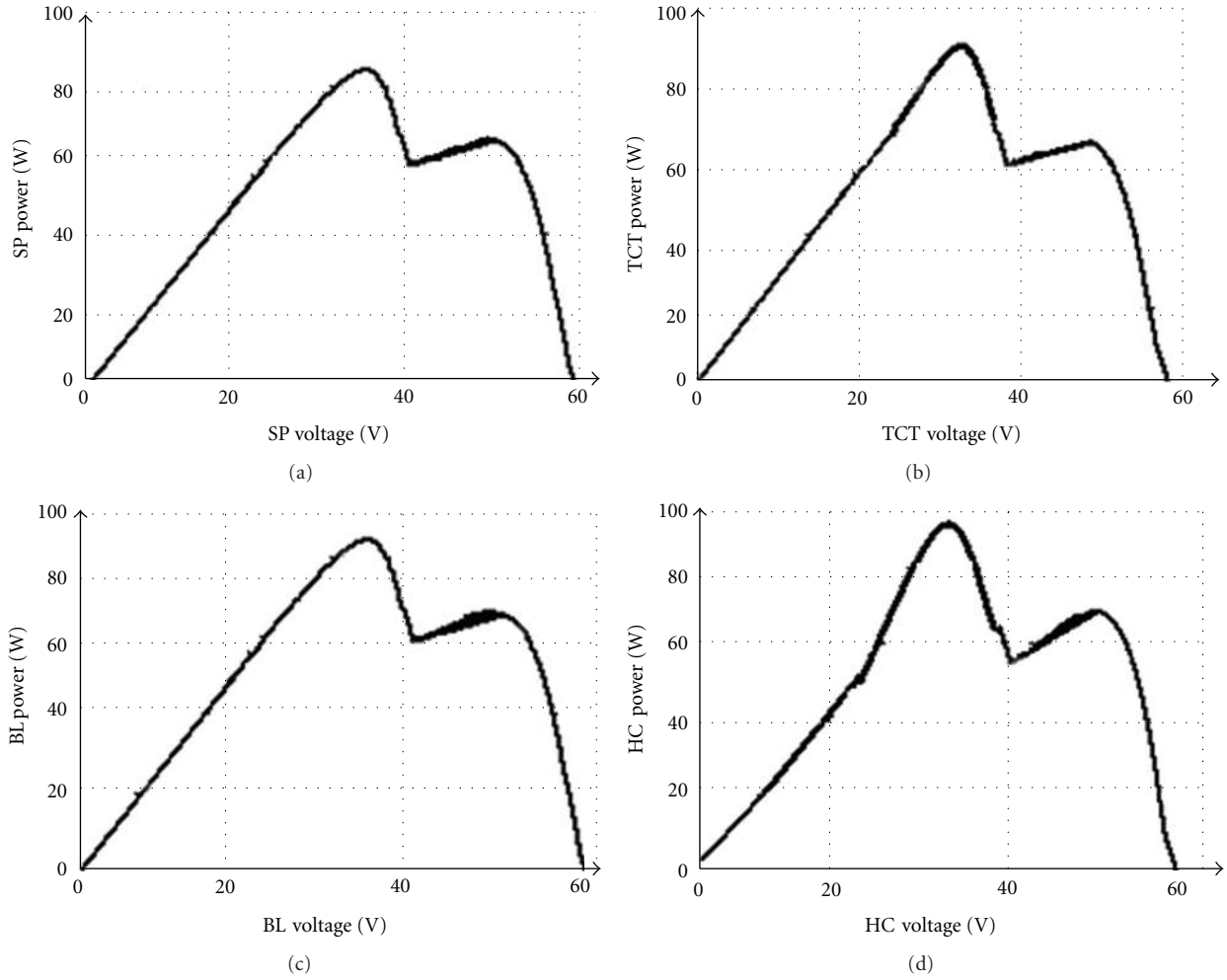

Figure 12: Calculated *P-V* characteristics for Figure 11.

Figure 13: 10 kW SPVA (14 × 10) installed in open terrace of EEE department block by SSNRC (BELL Laboratories).

trial and error method so as to match with the experimental characteristics. The values of "a" and "m" were found as 0.10 and −3.70, respectively. These values are used by proper multiplication factor for modelling SPV modules/arrays.

The parameters of the SOLKAR solar module used for practical verification at STC ($G = 1000$ W/m^2 and $T = 25^\circ$C) are given in Table 8.

Nomenclature

I_{PV}: Solar module output current (A)
V_{PV}: Solar module output voltage (V)
I_{ph}: Photo current of the SPV module (A)
I_r: Diode reverse saturation current in the equivalent circuit (μA)
R_{se}: Series resistance in the equivalent circuit of the module (mΩ)
R_{sh}: Parallel resistance in the equivalent circuit of the module (Ω)
n: Diode ideality factor
q: Electron charge (=1.602 × 10^{-19} C)
k: Boltzman's constant (= 1.381 × 10^{-23} J/K)
T: Temperature (Kelvin)
V_t: Thermal voltage (= nkT/q)
G: Irradiance level (at reference condition $G = 1000$ W/m^2)
α: Short-circuit current temperature coefficient
β: Open-circuit voltage temperature coefficient
I_{sc}: Short-circuit current of the module

V_{oc}: Open-circuit voltage of the module
V_m: Maximum power point voltage
I_m: Maximum power point current
P_m: Maximum power
ref: Additions subscripts indicate the parameters at reference conditions.

Index

SPVA: Solar photovoltaic array
SP: Series-parallel configuration
TCT: Total cross-tied configuration
BL: Bridge linked configuration
HC: Honey-Comb configuration
MPP: Maximum power point.

Acknowledgment

The authors wish to thank the management of the college for providing all the experimental and computational facilities to carry out this work.

References

[1] V. Quaschning and R. Hanitsch, "Numerical simulation of current-voltage characteristics of photovoltaic systems with shaded solar cells," *Solar Energy*, vol. 56, no. 6, pp. 513–520, 1996.

[2] J. H. R. Enslin, M. S. Wolf, D. B. Snyman, and W. Swiegers, "Integrated photovoltaic maximum power point tracking converter," *IEEE Transactions on Industrial Electronics*, vol. 44, no. 6, pp. 769–773, 1997.

[3] W. Herrmann, W. Wiesner, and W. Vaassen, "Hot spot investigations on PV modules - new concepts for a test standard and consequences for module design with respect to bypass diodes," in *Proceedings of the 26th IEEE Photovoltaic Specialists Conference*, pp. 1129–1132, October 1997.

[4] N. D. Kaushika and N. K. Gautam, "Energy yield simulations of interconnected solar PV arrays," *IEEE Transactions on Energy Conversion*, vol. 18, no. 1, pp. 127–134, 2003.

[5] M. Klenk, S. Keller, L. Weber et al., "Investigation of the hot-spot behaviour and formation in crystalline silicon Power cells, PV in Europe, From PV technology to energy solutions," in *Proceedings of the International Conference*, pp. 272–275, 2002.

[6] A. Woyte, J. Nijs, and R. Belmans, "Partial shadowing of photovoltaic arrays with different system configurations: literature review and field test results," *Solar Energy*, vol. 74, no. 3, pp. 217–233, 2003.

[7] H. S. Rauschenbach, "Electrical output of shadowed solar arrays," *IEEE Transactions on Electron Devices*, vol. 18, no. 8, pp. 483–490, 1971.

[8] M. C. Alonso-García, J. M. Ruiz, and W. Herrmann, "Computer simulation of shading effects in photovoltaic arrays," *Renewable Energy*, vol. 31, no. 12, pp. 1986–1993, 2006.

[9] M. C. Alonso-García, J. M. Ruiz, and F. Chenlo, "Experimental study of mismatch and shading effects in the I-V characteristic of a photovoltaic module," *Solar Energy Materials and Solar Cells*, vol. 90, no. 3, pp. 329–340, 2006.

[10] E. Karatepe, M. Boztepe, and M. Colak, "Development of suitable model for characterizing photovoltaic arrays with shaded solar cells," *Solar Energy*, pp. 329–340, 2007.

[11] R. Ramaprabha and B. L. Mathur, "Effect of shading on series and parallel connected solar PV modules," *Journal of Modern Applied Science*, vol. 3, no. 10, pp. 32–41, 2009.

[12] W. Xiao, N. Ozog, and W. G. Dunford, "Topology study of photovoltaic interface for maximum power point tracking," *IEEE Transactions on Industrial Electronics*, vol. 54, no. 3, pp. 1696–1704, 2007.

[13] T. Noguchi, S. Togashi, and R. Nakamoto, "Short-current pulse-based maximum-power-point tracking method for multiple photovoltaic-and-converter module system," *IEEE Transactions on Industrial Electronics*, vol. 49, no. 1, pp. 217–223, 2002.

[14] E. Román, R. Alonso, P. Ibañez, S. Elorduizapatarietxe, and D. Goitia, "Intelligent PV module for grid-connected PV systems," *IEEE Transactions on Industrial Electronics*, vol. 53, no. 4, pp. 1066–1073, 2006.

[15] N. Femia, G. Lisi, G. Petrone, G. Spagnuolo, and M. Vitelli, "Distributed maximum power point tracking of photovoltaic arrays: novel approach and system analysis," *IEEE Transactions on Industrial Electronics*, vol. 55, no. 7, pp. 2610–2621, 2008.

[16] L. Gao, R. A. Dougal, S. Liu, and A. P. Iotova, "Parallel-connected solar PV system to address partial and rapidly fluctuating shadow conditions," *IEEE Transactions on Industrial Electronics*, vol. 56, no. 5, pp. 1548–1556, 2009.

[17] R. Gules, J. D. P. Pacheco, H. L. Hey, and J. Imhoff, "A maximum power point tracking system with parallel connection for PV stand-alone applications," *IEEE Transactions on Industrial Electronics*, vol. 55, no. 7, pp. 2674–2683, 2008.

[18] C. Gonzalez and R. Weaver, "Circuit design considerations for photovoltaic modules and systems," in *Proceedings of the 14th IEEE Photovoltaic Specialist Conference*, pp. 528–535, January 1980.

[19] N. F. Shepard and R. S. Sugimura, "The integration of bypass diode with terrestrial photovoltaic modules and arrays," in *Proceedings of the 17th IEEE Photovoltaic Specialist Conference*, pp. 676–681, 1984.

[20] F. Giraud and Z. Salameh, "Analysis of the effects of a passing cloud on a grid-interactive photovoltaic system with battery storage using neural networks," *IEEE Transactions on Energy Conversion*, vol. 14, no. 4, pp. 1572–1577, 1999.

[21] Y. J. Wang and P. C. Hsu, "Analysis of partially shaded PV modules using piecewise linear parallel branches model," *World Academy of Science, Engineering and Technology*, vol. 60, pp. 783–789, 2009.

[22] Y. J. Wang and P. C. Hsu, "An investigation on partial shading of PV modules with different connection configurations of PV cells," *International Journal on Energy*, vol. 36, no. 5, pp. 3069–3078, 2011.

[23] M. G. Jaboori, M. M. Saied, and A. R. Hanafy, "A contribution to the simulation and design optimization of photovoltaic systems," *IEEE Transactions on Energy Conversion*, vol. 6, no. 3, pp. 401–406, 1991.

[24] W. T. Jewell and T. D. Unruh, "Limits on cloud-induced fluctuation in photovoltaic generation," *IEEE Transactions on Energy Conversion*, vol. 5, no. 1, pp. 8–14, 1990.

[25] H. Patel and V. Agarwal, "MATLAB-based modeling to study the effects of partial shading on PV array characteristics," *IEEE Transactions on Energy Conversion*, vol. 23, no. 1, pp. 302–310, 2008.

[26] H. Patel and V. Agarwal, "Maximum power point tracking scheme for PV systems operating under partially shaded conditions," *IEEE Transactions on Industrial Electronics*, vol. 55, no. 4, pp. 1689–1698, 2008.

[27] M. S. Swaleh and M. A. Green, "Effect of shunt resistance and bypass diodes on the shadow tolerance of solar cell modules," *Solar Cells*, vol. 5, no. 2, pp. 183–198, 1982.

[28] M. G. Villalva, J. R. Gazoli, and E. R. Filho, "Comprehensive approach to modeling and simulation of photovoltaic arrays," *IEEE Transactions on Power Electronics*, vol. 24, no. 5, pp. 1198–1208, 2009.

[29] S. Silvestre, A. Boronat, and A. Chouder, "Study of bypass diodes configuration on PV modules," *Applied Energy*, vol. 86, no. 9, pp. 1632–1640, 2009.

[30] R. Ramaprabha and B. L. Mathur, "Modelling and simulation of solar PV array under partial shaded conditions," in *Proceedings of the IEEE-International Conference on Sustainable Energy Technologies (ICSET '08)*, pp. 7–11, SMU Conference Centre, Singapore, November 2008.

[31] J. W. Bishop, "Computer simulation of the effects of electrical mismatches in photovoltaic cell interconnection circuits," *Solar Cells*, vol. 25, no. 1, pp. 73–89, 1988.

[32] M. C. Alonso-García and J. M. Ruíz, "Analysis and modelling the reverse characteristic of photovoltaic cells," *Solar Energy Materials and Solar Cells*, vol. 90, no. 7-8, pp. 1105–1120, 2006.